Available online at www.sciencedirect.com
SCIENCE DIRECT
Journal of Sound and Vibration 296 (2006) 73–90
JOURNAL OF SOUND AND VIBRATION
www.elsevier.com/locate/jsvi

Transfer function modeling of multi-link flexible structures

Yoram Halevi*, Clarice Wagner-Nachshoni

Faculty of Mechanical Engineering, Technion - Israel Institute of Technology, Haifa 32000, Israel

Received 21 January 2004; received in revised form 9 December 2005; accepted 31 January 2006
Available online 23 May 2006

Abstract

The paper considers the problem of deriving the accurate, infinite dimension, Laplace transfer function matrix of a system consisting of links that are individually governed by a one-dimensional wave equation. The first step is deriving some single input transfer functions, for a single uniform link. The building blocks of those transfer functions are time delays, representing the wave motion, and low-order rational expressions, representing the boundary phenomena. The transfer function approach enables simple yet accurate simulation schemes, exact frequency response for the entire frequency range, finite time analytical solutions, and a good starting point for dedicated control laws. The transfer function provides also an alternative way of obtaining many of the well-known properties of flexible structures. Three methods of modeling multi-link systems are presented. Two of them provide systematic and easy to use approaches for deriving models for systems of any order.

1. Introduction

Flexible structures are governed by partial differential equations (PDE), and hence have infinite dimension. However, most modeling methods use finite dimension approximations of the system. In the modal approach the infinite dimension appears as an infinite sum of spatial eigenfunctions multiplied by time functions. In practice though, only a finite sum is used. In the popular finite element method (FEM), the finite dimension is achieved by spatial discretization. While finite approximation is practically and even conceptually convenient, some important properties of the system's behavior are lost by it.

This paper takes a different approach. It considers the problem of deriving the accurate, infinite dimension, Laplace transfer function of a system consisting of links that are individually governed by a one-dimensional wave equation. It is assumed that the system is subjected to a finite number of point actuators (inputs), and that its behavior at a finite number of locations (outputs) is of interest. The first step is deriving a set of single input, infinite dimension, transfer functions for a single uniform link. The results, once properly rearranged, are in line with the wave approach to structures [1–5]. The building blocks of those transfer functions are time delays, representing the wave motion, and low-order rational expressions, representing the boundary phenomena.

*Corresponding author. Tel.: +972 4 8293465; fax: +975 4 8295711.
E-mail address: merhy01@tx.technion.ac.il (Y. Halevi).

0022-460X/$ - see front matter © 2006 Elsevier Ltd. All rights reserved.
doi:10.1016/j.jsv.2006.01.069

The transfer function modeling approach has several theoretical and practical advantages. Simple algebraic investigation of these transfer functions reveals many properties of the flexible links such as stability, rigid body degrees of freedom, and reciprocity. In the case of conservative boundary conditions this represents a different, and to the best of our knowledge new, way of obtaining well-known results from the modal approach. When the boundary conditions contain dampers, the results presented in this paper do not have counterparts in classical modal analysis. The practical opportunities offered by the transfer function approach are accurate yet simple simulation schemes, exact frequency response for the entire frequency range, analytical solution for the finite time response and identification of dedicated control laws.

The use of transfer functions to model flexible structures is not a new idea and results for some cases have been reported [6–13]. The problem is often expressed in terms of the Green's function of the system, since the transfer function is the Laplace transform of that function [9]. In some cases, e.g. Ref. [11], the results are in the spirit of the modal approach and the transfer functions are given as a sum of an infinite series of modal terms. In other cases, e.g. Ref. [6], closed form expressions were derived only for a free–free system. A general method, applicable to a wide range of systems, is presented in Ref. [12]. This method is based on a matrix exponent in the s domain. Numerous transfer functions have been derived in Ref. [8, Section 1.14], but the general boundary conditions case considered in this paper does not coincide with any of them.

The class of linear systems governed by a one-dimensional wave equation considered in this paper is admittedly limited. However, only in this case are the infinite dimension transfer functions directly related to the wave approach, or in more general terms, to the time response. This is due to the fact that the exponents in the solution are linear in the Laplace variable s, thus representing time shifts. In beams, on the other hand, the transfer functions include terms such as exponents of $\alpha s^{1/2}$, where α is a complex constant, which do not correspond to time-domain operators. In some works, e.g. Ref. [14], the wave motion in more general structures was considered, using Fourier based *spatial* transfer functions. It is suggested in Ref. [14] to use inverse FFT to obtain the time responses. While this is a viable alternative to other modeling methods such as FEM, it cannot provide insight into the system properties and the controller design. Concentrating on linear systems governed by a one-dimensional wave equation enables a complete analytical investigation and the design of a dedicated controller with a distinct structure.

Standard, model based, control strategies are difficult to apply to flexible structures mainly due to the very high dimension of the FEM or modal models, and the low damping in the system. Taking account of the delays, or wave motions, in the system can be advantageous for controller design [15]. The explicit, highly structured, and physically meaningful form of the transfer functions in this paper was used for the design of dedicated control laws [16–19] that achieve finite spectrum, plus delay. From a physical point of view, this is achieved by making the actuating end a sink for the returning wave. This concept can be extended beyond the class of systems addressed in this paper, and also to nonlinear systems. As long as the actuating end has linear boundary conditions, the same control law will absorb the incoming wave even if the rest of the structure contains nonlinearities. In more general cases a different control law will be needed, yet the same line of action is still possible. Recently the wave approach has been applied to control of discrete systems, consisting of lumped springs and masses, with promising results [20].

After obtaining a transfer function for a single link, the next step in the modeling process is constructing a model for a multi-link system, possibly with several actuation and measurement points. It should be noted that since the basic unit is a uniform link, a change in diameter, for example, is considered as another link. Three methods for constructing the multi-link model will be discussed. They range from algebraic methods, through recursive assembly of links in a feedback fashion, to the infinite dimension equivalent of a "dynamic stiffness matrix". As in the single link case, the multi-link transfer functions allow physical insight into the system and lead to convenient simulation schemes and suitable control laws [18].

The paper is organized as follows. In Section 2 the basic single link, point moment, transfer function, is derived. It is then extended to distributed moment, non-zero initial conditions, and other transfer function. In Section 3 the properties of the transfer functions and their physical interpretations are considered. Section 4 discusses possible applications of the transfer function model. Section 5 presents modeling methods for multi-link structures. The results are summarized and discussed in Section 6.

2. Modeling of a single link

2.1. The standard problem

As an illustration of a system governed by the wave equation, consider the system in Fig. 1 showing a uniform rod of length L subjected to a lumped torque moment $M(t)$ at the point $x = x_0$.

Assuming no internal damping, the torsional waves in the system are governed by the wave equation [4]:

$$\frac{1}{c^2}\frac{\partial^2\theta(x,t)}{\partial t^2} - \frac{\partial^2\theta(x,t)}{\partial x^2} = \frac{1}{GI_p}\cdot M(t)\cdot\delta(x-x_0), \tag{1}$$

where $\theta(x,t)$ is a torsion angle at distance x from the left end, I_p denotes the polar moment of inertia, ρ is the material density, G is the shear elasticity modulus, and $c = (G/\rho)^{1/2}$ is the wave propagation velocity. The boundary conditions are given by

$$\begin{aligned} I_pG\frac{\partial\theta(x,t)}{\partial x} &= J_1\frac{\partial^2\theta(x,t)}{\partial t^2} + D_1\frac{\partial\theta(x,t)}{\partial t} + K_1\theta(x,t), \quad x = 0,\\ I_pG\frac{\partial\theta(x,t)}{\partial x} &= -\left(J_2\frac{\partial^2\theta(x,t)}{\partial t^2} + D_2\frac{\partial\theta(x,t)}{\partial t} + K_2\theta(x,t)\right), \quad x = L, \end{aligned} \tag{2}$$

where J_i, D_i and K_i, $i = 1, 2$ are the inertia, damper and spring constant at an end. This general setting includes all linear boundary conditions of interest. For example, in a free end all the coefficients are identically zero, and a fixed end is obtained when $K \to \infty$ (or $J \to \infty$).

A Laplace transform with respect to time converts the PDE (1) into an ODE in x:

$$\frac{\partial^2\theta(x,s)}{\partial x^2} - \frac{s^2}{c^2}\theta(x,s) = -\frac{1}{GI_p}\cdot M(s)\delta(x-x_0), \tag{3}$$

where $M(s)$ and $\theta(x,s)$ denote Laplace transforms, with respect to time, of $M(t)$ and $\theta(x,t)$ respectively. The boundary conditions become

$$\begin{aligned} I_pG\frac{\partial\theta(x,s)}{\partial x} &= (J_1s^2 + D_1s + K_1)\theta(x,s), \qquad x = 0,\\ I_pG\frac{\partial\theta(x,s)}{\partial x} &= -(J_2s^2 + D_2s + K_2)\theta(x,s), \quad x = L. \end{aligned} \tag{4}$$

It is shown in Appendix A that the solution of Eq. (3) is

$$\theta(x,s) = -\frac{cM(s)}{4GI_ps}(e^{s|x-x_0|/c} - e^{-s|x-x_0|/c}) + C_1(s)e^{sx/c} + C_2(s)e^{-sx/c}. \tag{5}$$

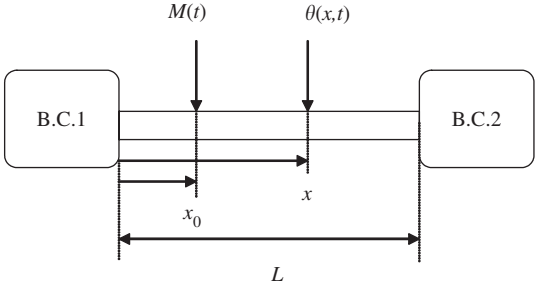

Fig. 1. The flexible system.

Substituting Eq. (5) into the boundary conditions (4) gives, after solving the two linear equations for $C_1(s)$ and $C_2(s)$ (see Appendix A for complete derivation), the following transfer function:

$$\frac{\theta(x,x_0,s)}{M(s)}=\begin{cases}\dfrac{1}{2\phi s}\cdot\dfrac{e^{-(\gamma-\delta)\tau s}+R_1(s)e^{-(\gamma+\delta)\tau s}+R_2(s)e^{-(2-\gamma-\delta)\tau s}+R_1(s)R_2(s)e^{-(2-\gamma+\delta)\tau s}}{1-R_1(s)R_2(s)e^{-2\tau s}}, & x\geqslant x_0,\\ \dfrac{1}{2\phi s}\cdot\dfrac{e^{-(\delta-\gamma)\tau s}+R_1(s)e^{-(\gamma+\delta)\tau s}+R_2(s)e^{-(2-\gamma-\delta)\tau s}+R_1(s)R_2(s)e^{-(2-\delta+\gamma)\tau s}}{1-R_1(s)R_2(s)e^{-2\tau s}}, & x\leqslant x_0,\end{cases} \tag{6}$$

where

$$\phi=\frac{GI_p}{c},\quad \tau=\frac{L}{c},\quad \gamma=\frac{x}{L},\quad \delta=\frac{x_0}{L}$$

and

$$R_i(s)=\frac{\phi s-(J_i s^2+D_i s+K_i)}{\phi s+(J_i s^2+D_i s+K_i)},\quad i=1,2. \tag{7}$$

The physical interpretation of these quantities will be discussed in Section 3. By defining

$$\beta=\frac{|x-x_0|}{L},\quad \eta=\frac{\max(x,x_0)}{L},$$

the two equations for the transfer function can be combined into the single expression

$$G(x,x_0,s)=\frac{1}{2\phi s}\cdot\frac{e^{-\beta\tau s}+R_1(s)e^{-(2\eta-\beta)\tau s}+R_2(s)e^{-(2-2\eta+\beta)\tau s}+R_1(s)R_2(s)e^{-(2-\beta)\tau s}}{1-R_1(s)R_2(s)e^{-2\tau s}}, \tag{8}$$

or equivalently

$$G(x,x_0,s)=\frac{1}{2\phi s}\cdot\frac{(1+R_1(s)e^{-2(\eta-\beta)\tau s})(1+R_2(s)e^{-2(1-\eta)\tau s})}{1-R_1(s)R_2(s)e^{-2\tau s}}e^{-\beta\tau s}. \tag{9}$$

The latter form emphasizes the pure delay of the system, which is $\beta\tau$, and is also convenient for the special cases given in Table 1.

2.2. Extensions-distributed moment and initial conditions

The fundamental transfer function derived in the previous subsection assumes that the external moment is applied at a point and that the initial conditions are zero. In general, the moment may be distributed, as shown in Fig. 2, and the initial conditions are given by $\theta(x,0)=\theta_0(x)$, $\partial\theta/\partial t(x,0)=\omega_0(x)$.

Table 1
Special cases of the transfer function

Case	$G(x,s)$
$x_0=0$	$\dfrac{1}{2\phi s}\cdot\dfrac{(1+R_1(s))(1+R_2(s)e^{-2(1-\beta)\tau s})}{1-R_1(s)R_2(s)e^{-2\tau s}}e^{-\beta\tau s}$
$x_0=x$	$\dfrac{1}{2\phi s}\cdot\dfrac{(1+R_1(s)e^{-2\eta\tau s})(1+R_2(s)e^{-2(1-\eta)\tau s})}{1-R_1(s)R_2(s)e^{-2\tau s}}$
$x_0=x=0$	$\dfrac{1}{2\phi s}\cdot\dfrac{(1+R_1(s))(1+R_2(s)e^{-2\tau s})}{1-R_1(s)R_2(s)e^{-2\tau s}}$
$x_0=0,\ x=L$	$\dfrac{1}{2\phi s}\cdot\dfrac{(1+R_1(s))(1+R_2(s))e^{-\tau s}}{1-R_1(s)R_2(s)e^{-2\tau s}}$

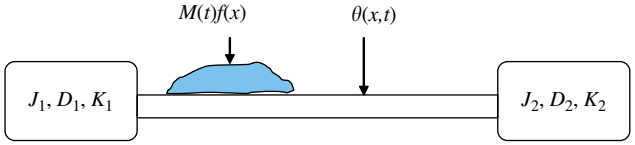

Fig. 2. A structure with distributed moment.

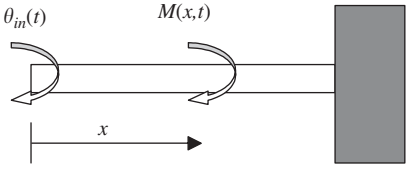

Fig. 3. A fixed–free system with an angle input.

A Laplace transform leads then to the following ODE:

$$\frac{\partial^2\theta(x,s)}{\partial x^2}-\frac{s^2}{c^2}\theta(x,s)=-\frac{1}{GI_p}\cdot M(s)f(x)-\frac{s}{c^2}\cdot\theta_0(x)-\frac{1}{c^2}\cdot\omega_0(x). \tag{10}$$

$\theta(x,s)$ can be derived by solving the equation, including its boundary conditions that are unchanged. However, treating the functions $f(x)$, $\theta_0(x)$ and $\omega_0(x)$ as weighted infinite sums of delta functions, it is easier to use the convolution, or Green function [9] integral

$$\theta(x,s)=M(s)\int_0^L G(x,x_0,s)f(x_0)\,\mathrm{d}x_0+s\rho I_p\int_0^L G(x,x_0,s)\theta_0(x_0)\,\mathrm{d}x_0+\rho I_p\int_0^L G(x,x_0,s)\omega_0(x_0)\,\mathrm{d}x_0. \tag{11}$$

The identity $\rho=G/c^2$ was used in the last two terms. Numerical integration can be used if no analytic expression exists for the integral, or equivalently for the differential equation (10). Even though the moment is distributed, $M(t)$ is a scalar and one can obtain the SISO transfer function from $M(s)$ to $\theta(x,s)$ as

$$\frac{\theta(x,s)}{M(s)}=\int_0^L G(x,x_0,s)f(x_0)\,\mathrm{d}x_0. \tag{12}$$

2.3. Some other transfer functions

Next we consider a similar problem that is required for the dynamic stiffness approach for multiple-link modeling in Section 5. Consider the system in Fig. 3, where a flexible link is fixed at one end and is rotated by an angle $\theta_{\mathrm{in}}(t)$ at the other.

This time we are interested in the transfer function from the input angle θ_{in} to the moments in the rod. The system is still governed by the one-dimensional wave equation (1), but the boundary conditions change to

$$\theta(0,t)=\theta_{\mathrm{in}}(t),\quad \theta(L,t)=0. \tag{13}$$

A derivation similar to the previous case leads to

$$K_c(s)=\frac{M(0,s)}{\theta_{\mathrm{in}}(s)}=\frac{\phi s(1+e^{-2\tau s})}{1-\mathrm{e}^{-2\tau s}}, \tag{14}$$

$$K_{\mathrm{nc}}(s)=\frac{M(L,s)}{\theta_{\mathrm{in}}(s)}=\frac{2\phi s\mathrm{e}^{-\tau s}}{1-\mathrm{e}^{-2\tau s}}. \tag{15}$$

Here the subscripts 'c', and 'nc', stand for collocated and non-collocated, respectively.

Some methods of multi-link modeling, which will be presented in the sequel, give only the angles at the ends of a flexible rod. The angle at any point along the rod is then given by

$$\theta(x,s)=\frac{e^{-\gamma\tau s}-e^{-(2-\gamma)\tau s}}{1-e^{-2\tau s}}\theta(0,s)+\frac{e^{-(1-\gamma)\tau s}-e^{-(1+\gamma)\tau s}}{1-e^{-2\tau s}}\theta(L,s). \tag{16}$$

3. Physical interpretation of the transfer function

The transfer function (8) was derived in a straightforward mathematical manner, but it has a distinct structure that corresponds to a clear and meaningful physical interpretation. These properties are analyzed in this section, and their applications are given in Section 4.

3.1. Delays and the wave approach

Since c is the wave propagation velocity, τ is the time required for the wave to travel from one end to another, and can be regarded as the time constant of the structure. The numerator of $G(x,x_0,s)$ contains four exponents with negative argument, which are time delays. They represent the four possible routes of the wave from x_0 to x, without completing a full cycle, and are shown in Fig. 4 for $x>x_0$. The shortest route is clearly the direct one, and it is the pure time delay existing in the system, as can be seen from Eq. (9).

$R_i(s)$ are dynamic reflection coefficients of the motion at each end. Some important special cases are of interest. If the end is free, then $R_i(s)=1$ and the wave is returned identically. A fixed end is obtained by $K_i\to\infty$ (equivalently $J_i\to\infty$), which results in $R(s)=-1$. The wave is then returned identically but with a changed sign. If the end contains no damper, then it follows immediately that $R_i(s)R_i(-s)=1$ and consequently $|R_i(j\omega)|=1$. This property is an indication of conservation of energy, which exists in systems without dampers.

A transfer function that is based on delays, representing the wave motion along the flexible link, and dynamic reflection coefficients, describes the system in terms of the moving wave approach. This is a major departure from the modal approach where the moving waves are described as an infinite sum of standing waves.

3.2. Relationship with classical vibration theory

While the approach in this paper is different from the classical vibration theory, e.g. Refs. [4,21], all the results of the latter can be recovered from the transfer function (8). This sub-section is devoted to showing those well-known results from a different point of view, and to demonstrate the wealth of information included in the transfer function (8). The results are given here in a brief manner and elaborated derivation and discussion of them can be found in Ref. [19].

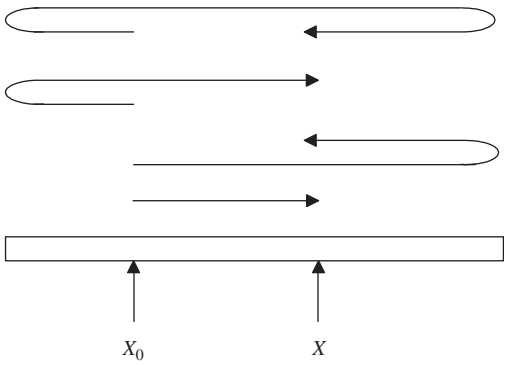

Fig. 4. The four time delays in $G(x,s)$.

Reciprocity: The transfer function does not change if the actuation and measurement points are interchanged. This is immediate from the fact that η and β remain the same.

Eigenvalues: The eigenvalues of the system in all possible cases are the roots of the characteristic equation

$$1 - R_1(s)R_2(s)\mathrm{e}^{-2\tau s} = 0. \tag{17}$$

In conservative systems, where $|R_i(\mathrm{j}\omega)| = 1$, the roots are purely imaginary and only the phase angle has to be considered. The natural frequencies in that case are the solutions of

$$\tan^{-1}\frac{\phi\omega_k}{K_1 - J_1\omega_k^2} + \tan^{-1}\frac{\phi\omega_k}{K_2 - J_2\omega_k^2} + \tau\omega_k = k\pi. \tag{18}$$

This equation is different and more explicit than the one usually used in classical control texts. For example it reveals immediately that if both ends contain inertia then as k increases, $\omega_k \to (k-2)\pi/\tau$. In case only one end contains inertia, with or without a spring, and the other end contains only a spring, then as k increases, $\omega_k \to (k-3/2)\pi/\tau$, etc. It is worth noting that Eq. (18) is in accordance with the phase closure principle, which exists in conservative systems [22].

Stability: The following observations are proven in Appendix B by considering the characteristic equation (17).

(a) The system does not have poles (eigenvalues) in the open right half-plane (ORHP) for all possible values of the inertia, spring constant and damping, including zero.
(b) If at least one of the damping elements D_i is non-zero then the system has one pole at the origin (if no springs exist) and all other poles are in the OLHP.
(c) In the absence of damping all the poles are on the imaginary axis (natural frequencies).

Poles at the origin (*rigid body modes*): The transfer function (8) has two poles at the origin if the boundary conditions consist of inertias only, one pole if there exists at least one damper (but no springs), and no such poles if there exists at least one spring.

3.3. Comparison with finite dimension models

A common way of modeling flexible structures, mainly for conservative systems, is expressing $\theta(x,t)$ as

$$\theta(x,t) = \sum_{k=1}^{N} V_k(x)q_k(t) \tag{19}$$

for a certain finite N. This approximation leads to a state space model of order $n = 2N$. If the spatial functions $V_k(x)$ are the exact modeshapes of the system, then Eq. (19) represents the modal truncation method. This form can be obtained directly from Eq. (8) by writing

$$G(x,s) = \frac{c_{00}(x)}{s^2} + \frac{c_0(x)}{s} + \sum_{k=1}^{\infty}\left(\frac{c_k(x)}{s-p_k} + \frac{\bar{c}_k(x)}{s-\bar{p}_k}\right). \tag{20}$$

The existence of the first two terms depends on the number of poles at the origin, and p_k are the poles of the system, i.e. the roots of Eq. (17). The coefficients $c_k(x)$ are given by

$$c_k(x) = \lim_{s\to p_k}(s-p_k)G_\theta(x,s). \tag{21}$$

By writing $G(x,x_0,s)$, with obvious notation, as

$$G(x,x_0,s) = \frac{N(x,s)}{2\phi s D(s)}, \tag{22}$$

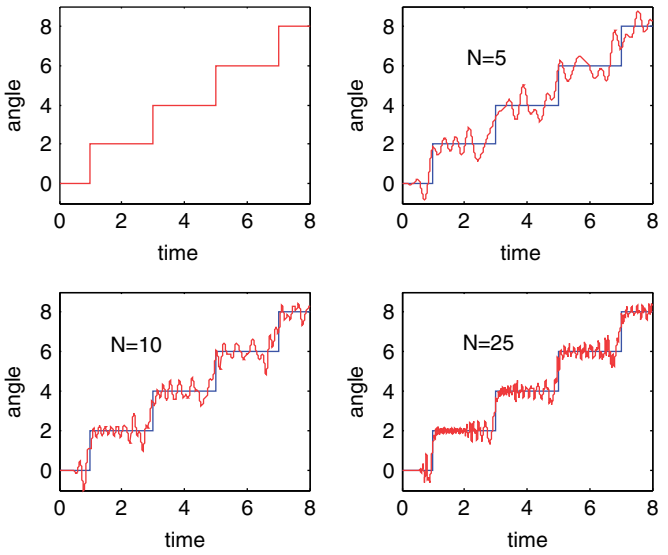

Fig. 5. Impulse response of the true system (top left) and three FEM models with 5, 10 and 25 elements. The moment $M(t)$ acts on the left end, the normalized angle is $2\phi \cdot \theta(L)$ and the normalized time is t/τ.

we can obtain, using L' hôpital's principle, explicit expressions for $c_k(x)$:

$$c_k(x) = \frac{N(x,p_k)}{2\phi p_k D'(p_k)} = \frac{N(x,p_k)}{2\phi p_k \left(2\tau - \frac{R_1'(p_k)}{R_1(p_k)} - \frac{R_2'(p_k)}{R_2(p_k)}\right)}. \tag{23}$$

In Eq. (23) "′" denotes derivative with respect to s. In the absence of any spring (otherwise $s = 0$ is not a pole), formal derivation leads to the following expected expressions for $c_{00}(x)$ and $c_0(x)$.

$$c_{00}(x) = \begin{cases} \frac{1}{J_1+J_2+J_r}, & D_1 = D_2 = 0 \\ 0 & \text{otherwise} \end{cases}, \quad c_0(x) = \begin{cases} 0 & D_1 = D_2 = 0, \\ \frac{1}{D_1+D_2} & \text{otherwise.} \end{cases} \tag{24}$$

Here $J_r = \rho I_p L$ is the moment of inertia of the rod itself. Taking N terms of the series, one gets, for any given x, the same transfer function that would have been obtained by calculating the eigenvalues and eigenfunctions of the system and transforming it to modal coordinates.

If the spatial functions $V_k(x)$ are admissible functions satisfying the geometrical boundary conditions, then Eq. (19) represents the assumed mode method. The FEM can be regarded as a special case of the latter method when $V_k(x)$ have a certain structure with a local support. While the finite approximation methods are fairly accurate (absolutely accurate in case of modal truncation) in approximating the natural frequencies, the models do not posses a direct relationship with the delay. This is due to the fact that the delay is not related to a single mode (spatial function) or to a group of modes, but is a consequence of all the modes acting together. As the delay, or wave, is a key element of the structure's motion, invaluable insight is lost when one refers to finite dimension modeling.

The impulse response at the free end of a free–free rod subjected to a torque at the other end is shown in Fig. 5, together with three FEM approximations. As can be seen, even a system of order 50 is not capable of approaching the true response. Notice also that although all the poles are purely imaginary, the true response is not oscillatory. The oscillations in the approximations are thus artifacts of modeling and are not related to the physical behavior.

4. Applications of the transfer function

The distinct structure of the transfer function leads to several applications and insights that cannot be obtained by standard modal and FEM modeling.

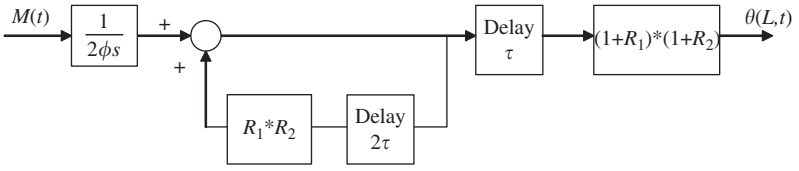

Fig. 6. A simulation scheme for the angle at $x = L$.

4.1. Simulation

Treating the denominator of $G(x,x_0,s)$ as if it is a result of feedback, we arrive at a simple simulation scheme consisting only of delays and linear second-order blocks, as is shown in Fig. 6. Standard simulation software, e.g. Simulink, can now be easily used to obtain an accurate time response at any number of points along the flexible link, as a result of different excitation conditions. This approach is much more efficient than numerical solution of the PDE. As was already demonstrated, finite dimension approximations such as FEM or truncated modal model often perform poorly in the time domain.

4.2. Analysis and design of damping elements

The effect of damping on the structure response is often of interest [23,24]. Modal approaches cannot handle lumped dampers at the ends, and FEM models give only an approximation. The characteristic equation (17) is convenient for analyzing the damping effect and can be useful in the design of such devices. The following simple example demonstrates this possibility.

Example 1: Consider a free–free rod and two dampers with constant D. One option, which will be called case I, is to put one damper on each side. The other option, denoted case II, is to put both of them in parallel on one side, which is equivalent to a single damper with a constant $2D$. The question is which configuration will provide more damping to the system. Calculating the reflection coefficients $R_i(s)$ for each case we obtain,

$$R_{1,\mathrm{I}} = R_{2,\mathrm{I}} = \frac{1-d}{1+d}, \quad R_{1,\mathrm{II}} = \frac{1-2d}{1+2d}, \quad R_{2,\mathrm{II}} = 1.$$

Here $d = D/\phi$ is the non-dimensional damping. The characteristic equation in this case is

$$1 - R_1 R_2 \mathrm{e}^{-2\tau s} = 0.$$

leading to the following sets of poles:

$$\mathrm{Re}\{p_{k,\mathrm{I}}\} = \tfrac{1}{\tau}\ln\left(\tfrac{|1-d|}{1+d}\right), \quad \mathrm{Im}\{p_{k,\mathrm{I}}\} = \tfrac{\pi k}{\tau},$$

$$\mathrm{Re}\{p_{k,\mathrm{II}}\} = \tfrac{1}{2\tau}\ln\left(\tfrac{|1-2d|}{1+2d}\right), \quad \mathrm{Im}\{p_{k,\mathrm{II}}\} = \begin{cases} \frac{\pi k}{\tau}, & d<1, \\ \frac{\pi(k-1/2)}{\tau}, & d>1. \end{cases}$$

Several interesting observations can be made. The real part is common to all poles, a property called uniform damping [24]. There are critical values, $d = 1$ in case I and $d = \frac{1}{2}$ in case II, where the poles go to infinity and the end becomes a sink for the wave. Beyond those values, increasing the damper constant results in decreased damping (real part) until as d approaches infinity the systems have no damping at all. In case I the damped natural frequencies (imaginary part) do not change with d while in case II this is true except for a jump at $d = \frac{1}{2}$. Finally, to answer the question in the beginning of the example, Fig. 7 shows that in the relevant range of $d < \frac{1}{2}$, configuration II, i.e. the two dampers in one side, results in poles with larger absolute value of the real part and hence with faster decay.

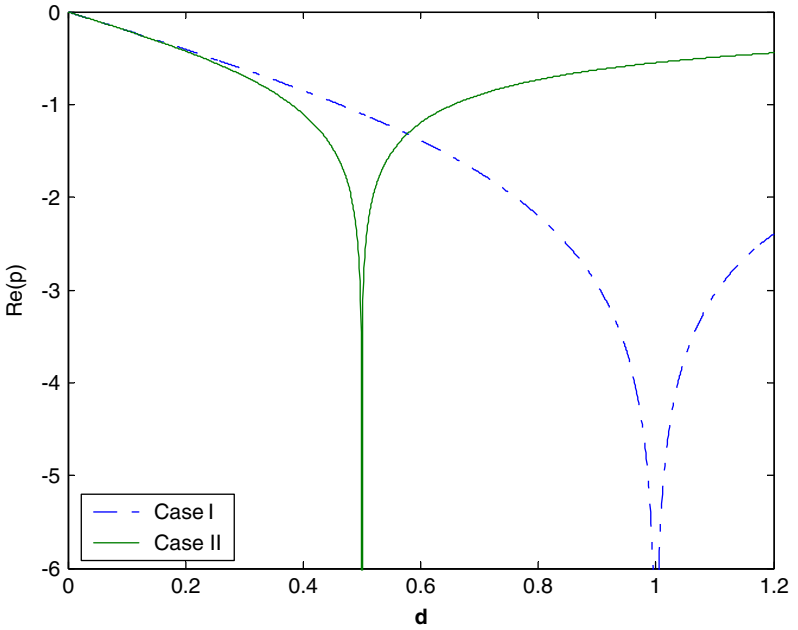

Fig. 7. The real part of the modes vs. the normalized damper constant $d = D/\phi$. Case I—dashed, case II—solid.

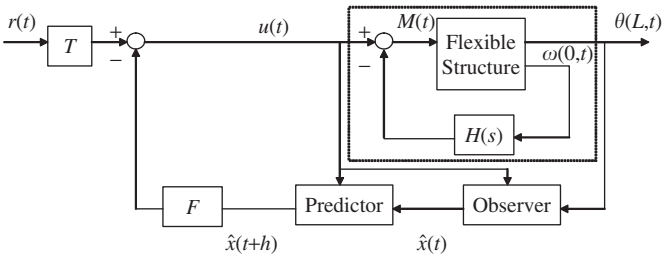

Fig. 8. Position tracking control scheme for a flexible link.

4.3. Time and frequency responses

Analytical solution: Using long division, $G(x, x_0, s)$ can be written as

$$G(x, x_0, s) = \sum_{k=0}^{\infty} \sum_{i=1}^{4} [R_1(s)R_2(s)]^k P_i(s) e^{-(h_i+2k)\tau s}, \tag{25}$$

where $P_i(s)$ and h_i correspond to the appropriate term of the numerator, e.g. $P_2(s) = R_1(s)$, $h_2 = 2\eta - \beta$. Suppose now that a solution is required only for $[0, T]$, then there is no need to consider the terms with delays greater than T, and an equivalent transfer function is given by a finite series. As each term represents a delayed linear system, an exact analytical solution can be obtained for any input.

Frequency response: The exact frequency response function (FRF) for the entire frequency range is obtained by simply calculating $G(x, x_0, j\omega)$. All finite approximations give the FRF only in a finite frequency band. It should be noted that truncated modal models have the correct natural frequencies, but not the accurate frequency response even at the range of frequency included in the model.

4.4. Feedback control design

The exact and explicit form of the transfer function can be used for the design of the feedback tracking control system shown in Fig. 8. This is the subject of several papers, e.g. Refs. [16,19], and will be discussed here only briefly.

Consider the collocated rate feedback, which is the inner loop in Fig. 8.

$$M(s) = u(s) - \frac{2\phi R_1(s)}{1 + R_1(s)}\omega(0, s). \tag{26}$$

By using that control law the delay is eliminated from the characteristic function and the closed loop transfer function from the command $u(s)$ to the displacement at $x = L$, the point of the outer feedback, is

$$\frac{\theta(L, s)}{u(s)} = \frac{1 + R_2(s)}{2\phi s} e^{-\tau s} = \frac{e^{-\tau s}}{J_2 s^2 + (D_2 + \phi)s + K_2}. \tag{27}$$

In the absence of inertia, the control law (26) reduces to a constant rate feedback, hence it can be considered as a generalization of the cases discussed in Example 1. The elimination of the poles is achieved when the end becomes a sink for the wave. Having the form of a rational transfer function plus delay, dead time compensators [25] can be used in the outer, position loop. The overall transfer function becomes then rational, with arbitrarily assigned dynamics, plus delay.

5. Modeling of multi-link systems

5.1. Problem statement

In the previous sections the transfer function model of a single link was derived, analyzed and discussed. Many structures consist of combinations of flexible links, and therefore a transfer function for more complex systems is sought. In this section, we extend the results obtained for a single link to a structure consisting of multiple links. We consider the case of N inertias connected by $N-1$ flexible rods shown in Fig. 9.

Each inertia J_k is connected to a constant frame (skyhook) with a spring K_k and a dashpot D_k, and is subjected to an external moment M_k. Some or all of those quantities may be zero, and the "inertia" k actually represents any kind of discontinuity, e.g. a change in the rod diameter. In Section 2, we derived the relationship between the angle at a general point along a link and the two angles at the ends. Therefore, it is sufficient to derive the transfer function from an input torque to the principal angles $\theta_i(t)$. In the following subsections we present three different approaches for this modeling problem. The first one, the direct algebraic approach is the most obvious way of approaching the problem, and is given here mainly for comparison with the other two that seem to be more promising.

5.2. Direct algebraic approach

The first method is algebraic, consisting of writing a separate PDE for each link and combining them through the boundary conditions. This approach is similar to common procedures in time domain [26], yet it is in the Laplace domain. It follows the same steps as for a single link, but for a set of equations. We present

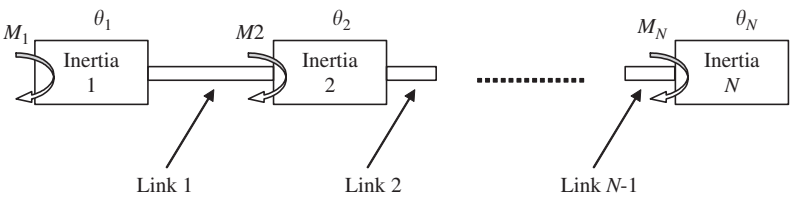

Fig. 9. A flexible multi-link system.

details for a two-link system, which is governed by two wave equations, shown already in the s domain

$$\frac{\partial^2\theta_i(x_i,s)}{\partial x_i^2}-\frac{s^2}{c_i^2}\theta_i(x_i,s)=0,\quad i=1,2, \tag{28}$$

where $\theta_i(x_i,s)$ is a torsion angle at distance x_i from the left end of each flexible rod. ρ_i, G_i, c_i and I_{pi}, $i=1,2$ are defined as before. The boundary conditions are given by

$$\begin{aligned}
&G_1I_{P1}\frac{\partial\theta_1}{\partial x_1}(0,s)=\left(J_1s^2+D_1s+K_1\right)\theta_1(0,s)-M(s),\\
&G_2I_{P2}\frac{\partial\theta_2}{\partial x_2}(L_2,s)=-\left(J_3s^2+D_3s+K_3\right)\theta_2(L_2,s),\\
&\theta_1(L_1,s)=\theta_2(0,s),\\
&G_2I_{P2}\frac{\partial\theta_2}{\partial x_2}(0,s)-G_1I_{P1}\frac{\partial\theta_1}{\partial x_1}(L_1,s)=\left(J_2s^2+D_2s+K_2\right)\theta_2(0,s).
\end{aligned} \tag{29}$$

The solution of Eq. (28) is given by

$$\theta_i(x_i,s)=C_{i1}(s)\cdot e^{sx_i/c_i}+C_{i2}(s)\cdot e^{-sx_i/c_i},\quad i=1,2. \tag{30}$$

The next step is substituting Eq. (30) into the boundary conditions and solving the four linear equations for the 'constants' $C_{ij}(s)$. Since the only non-homogeneous term is $M(s)$, all of these functions are proportional to it. After some lengthy derivation and rearranging, one arrives at the following transfer functions:

$$\frac{\theta_1(x_1,s)}{M(s)}=\frac{(B_0(s)+B_1(s)e^{-2(1-\beta_1)\tau_1 s}+B_2(s)e^{-2\tau_2 s}+B_3(s)e^{-2(\tau_1+\tau_2-\beta_1\tau_1)s})\cdot e^{-\beta_1\tau_1 s}}{s\cdot(A_0(s)+A_1(s)e^{-2\tau_1 s}+A_2(s)e^{-2\tau_2 s}+A_3(s)e^{-2(\tau_1+\tau_2)s})} \tag{31}$$

$$\frac{\theta_2(x_2,s)}{M(s)}=\frac{C_1(s)e^{-(\tau_1+\beta_2\tau_2)s}+C_2(s)e^{-(\tau_1+2\tau_2-\beta_2\tau_2)s}}{s\cdot(A_0(s)+A_1(s)e^{-2\tau_1 s}+A_2(s)e^{-2\tau_2 s}+A_3(s)e^{-2(\tau_1+\tau_2)s})}. \tag{32}$$

Here

$$\phi_i=\frac{G_iI_{pi}}{c_i},\quad \tau_i=\frac{L_i}{c_i},\quad \beta_i=\frac{x_i}{L_i},\quad i=1,2$$

and $A_i(s)$, $B_i(s)$ and $C_i(s)$ are polynomials whose explicit form is not shown here for the sake of brevity. Similar to a single link, long division of the numerator of Eq. (31) by its denominator leads to an infinite sum of delayed rational transfer functions. Fig. 10 shows some of the first delays. The physical interpretation is that each time the wave arrives at the discontinuity point, part of it moves in the same direction while another part is reflected back.

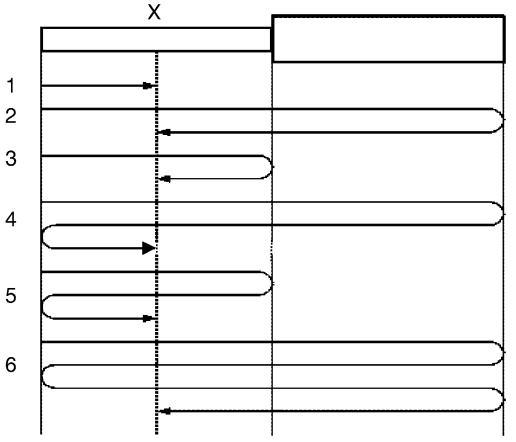

Fig. 10. The first routes (time delays) of the moment to a point in the first link.

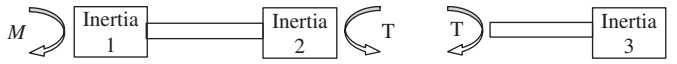

Fig. 11. The left and right subsystems.

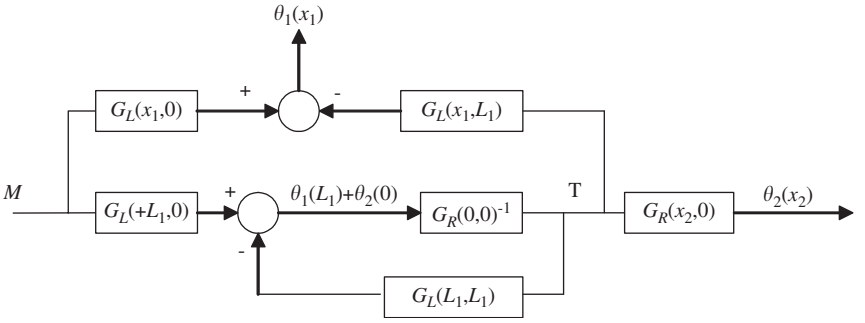

Fig. 12. Block diagram of the feedback connection.

5.3. Feedback approach

While the derivation in the previous subsection is certainly valid, and using it we were able to obtain the required transfer functions, it suffers from some drawbacks. First, the complexity of the expressions makes it difficult to identify any underlying structure. Secondly, extending the results to a larger number of links does not look promising.

In this subsection a different approach is taken. The system is partitioned into several smaller subsystems, and the model is constructed by using the correct interrelations existing between them. Applying that approach to a two-link system, the first step is to artificially disconnect the right flexible rod from the left subsystem and replace it by two torques with magnitude $T(t)$ acting on the two substructures in opposite directions. As a result we obtained two one-link subsystems, as shown in Fig. 11.

The left subsystem has inertia 1 and inertia 2 as its boundaries. Its transfer functions, denoted by $G_L(x_{10}, x_1, s)$ are given by Eq. (8) with ϕ_1, τ_1, and β_1 replacing ϕ, τ, and β, respectively. The right subsystem has a free left boundary condition and inertia 3 on its right end. Hence its transfer functions, denoted by $G_R(x_{20}, x_2, s)$ are given by Eq. (8) with ϕ_2, τ_2, β_2, 1 and R_3(s) replacing ϕ, τ, β, $R_1(s)$, and $R_2(s)$, respectively, where $R_3(s)$ is defined as

$$R_3(s) = \frac{\phi_2 s - \left(J_3 s^2 + D_3 s + K_3\right)}{\phi_2 s + (J_3 s^2 + D_3 s + K_3)}. \tag{33}$$

The torque $T(t)$ reflects the restoring action of the right subsystem when an angle input is applied to it. The overall motion in the left subsystem is a superposition of the responses to both $M(t)$ and $T(t)$. This procedure leads to the block diagram in Fig. 12.

Notice that all the transfer functions in the figure are similar to the cases listed in Table 1. Direct calculating yields

$$\begin{aligned}\frac{\theta_1(x_1,s)}{M(s)} &= G_L(x_1,0,s) - \frac{G_L(x_1,L_1,s)G_R(0,0,s)^{-1}G_L(0,L_1,s)}{1+G_R(0,0,s)^{-1}G_L(L_1,L_1,s)} \\ &= \frac{G_L(x_1,0,s)G_R(0,0,s) + G_L(x_1,0,s)G_L(L_1,L_1,s) - G_L(x_1,L_1,s)G_L(0,L_1,s)}{G_R(0,0,s)+G_L(L_1,L_1,s)},\end{aligned} \tag{34}$$

$$\begin{aligned}\frac{\theta_2(x_2,s)}{M(s)} &= \frac{G_R(x_2,0,s)G_R(0,0,s)^{-1}G_L(0,L_1,s)}{1+G_R(0,0,s)^{-1}G_L(L_1,L_1,s)} \\ &= \frac{G_R(x_2,0,s)G_L(0,L_1,s)}{G_R(0,0,s)+G_L(L_1,L_1,s)}.\end{aligned} \tag{35}$$

Explicit evaluation of the expressions in Eqs. (34) and (35) verifies that they are indeed identical with those in Eqs. (31) and (32). If the structure contains more than two links the process is repeated with the new disconnection point just before the last link, and the left subsystem is the entire system in Fig. 11. It is also possible to use larger subsystems on the right. For example, combining two two-link systems, whose transfer functions have already been calculated, yields the one for four links. Thus, using the feedback approach one can systematically find the exact, infinite dimensional, transfer function of a flexible system with any number of links.

Example 2: Consider a system with three identical mass moments of inertia J, connected by two identical links. The characteristic equation, given by the denominator of Eqs. (34) and (35) becomes

$$\begin{aligned}0 &= 2\phi s\left(1-R^2(s)\mathrm{e}^{-2\tau s}\right)\left(1+R(s)\mathrm{e}^{-2\tau s}\right)+\phi s(1+R(s))\left(1+R(s)\mathrm{e}^{-2\tau s}\right)\left(1-R(s)\mathrm{e}^{-2\tau s}\right)\\ &= \phi s\left(3+R(s)+\left(2R(s)-2R^2(s)\right)\mathrm{e}^{-2\tau s}-\left(R(s)+3R^2(s)\right)\mathrm{e}^{-4\tau s}\right)\\ &= \phi s(1+R(s)e^{-2\tau s})\left(1-\frac{R(s)+3R^2(s)}{3+R(s)}\mathrm{e}^{-2\tau s}\right)\\ &= \phi s\left(1+\frac{\phi-Js}{\phi+Js}\mathrm{e}^{-2\tau s}\right)\left(1-\frac{\phi-Js}{\phi+Js}\frac{2\phi-Js}{2\phi+Js}\mathrm{e}^{-2\tau s}\right).\end{aligned}$$

The first term is the pole at the origin, existing whenever the system does not have springs. The second is identical with the characteristic equation of a link clamped in one end, which indeed contains all the anti-symmetric modes of the system. The third term gives all the symmetric modes. Following the analysis in Appendix B it can be shown that all the poles are purely imaginary (also obvious since the system is conservative). Furthermore, the two expressions multiplying the exponents have unity absolute value for $s=\mathrm{j}\omega$. Hence the set of natural frequencies contains all ω that satisfy either one of the following equations:

$$\tan^{-1}(J\omega_k/\phi)+\tau\omega_k=(k+1/2)\pi,$$

$$\tan^{-1}(J\omega_m/\phi)+\tan^{-1}(J\omega_m/2\phi)+\tau\omega_m=m\pi.$$

These equations provide a much more convenient way of finding the natural frequencies for this three mass system than the one from classical vibration theory that is implicit.

5.4. Dynamic stiffness approach

The basic unit in the feedback approach in the previous section is a link together with its boundaries, and the model was obtained by combining links. A different approach is to consider the inertias as the 'main' elements and looking at the links as connections between them. Applying Newton's second law to the kth inertia in Fig. 9, we have

$$J_k\frac{\mathrm{d}^2\theta_k}{\mathrm{d}t^2}=-D_k\frac{\mathrm{d}\theta_k}{\mathrm{d}t}-K_k\theta_k+M_k+T_{k-1,k-1}+T_{k-1,k}+T_{k,k+1}+T_{k,k}. \tag{36}$$

Here

$T_{k-1,k-1}$ is the moment applied to J_k by link $k-1$ as a result of the angle θ_{k-1} when θ_k is fixed.
$T_{k-1,k}$ is the moment applied to J_k by link $k-1$ as a result of the angle θ_k when θ_{k-1} is fixed.
$T_{k,k+1}$ is the moment applied to J_k by link k as a result of the angle θ_{k+1} when θ_k is fixed.
$T_{k,k}$ is the moment applied to J_k by link k as a result of the angle θ_k when θ_{k+1} is fixed.

Notice that if the links were modeled as pure springs, $T_{k-1,k-1}+T_{k-1,k}=K(\theta_{k-1}-\theta_k)$, and the same for the other link. Hence Eq. (36) is a generalization of the standard mass–spring modeling method. The role of of $K_c(s)$ and $K_{\mathrm{nc}}(s)$ in Eqs. (14) and (15) is revealed now, since they generate the four moments $T_{i,j}$. The index k, or $k-1$, in the following formulas denotes the links to which these transfer function belong. Notice that these are properties of the link, and due to symmetry are the same when $\theta_k(t)$ is fixed and $\theta_{k+1}(t)$ is the input. The

Laplace transform of Eq. (36) can be written as

$$A_k(s)\theta_k(s) = M_k(s) + K_{k-1,\mathrm{nc}}(s)\theta_{k-1}(s) - K_{k-1,c}(s)\theta_k(s) + K_{k,\mathrm{nc}}(s)\theta_{k+1}(s) - K_{k,c}(s)\theta_k(s). \tag{37}$$

$K_{0,c}(s) = K_{N,c}(s) = 0$, since the end inertias have only one flexible connection, and

$$A_k(s) = J_k s^2 + D_k s + K_k.$$

After rearranging Eq. (37) can be written as

$$-K_{k-1,\mathrm{nc}}(s)\theta_{k-1}(s) + (A_k(s) + K_{k-1,c}(s) + K_{k,c}(s))\theta_k(s) - K_{k,\mathrm{nc}}(s)\theta_{k+1}(s) = M_k(s). \tag{38}$$

Using the definition

$$S_k(s) = A_k(s) + K_{k-1,c}(s) + K_{k,c}(s).$$

the overall system is now given by

$$\begin{bmatrix} S_1(s) & -K_{1,\mathrm{nc}}(s) & 0 & \cdots & 0 \\ -K_{1,\mathrm{nc}}(s) & S_2(s) & -K_{2,\mathrm{nc}}(s) & 0 & \vdots \\ 0 & -K_{2,\mathrm{nc}}(s) & S_3(s) & \ddots & 0 \\ \vdots & 0 & \ddots & \ddots & -K_{N-1,\mathrm{nc}}(s) \\ 0 & \cdots & 0 & -K_{N-1,\mathrm{nc}}(s) & S_N(s) \end{bmatrix} \begin{bmatrix} \theta_1(s) \\ \theta_2(s) \\ \theta_3(s) \\ \vdots \\ \theta_N(s) \end{bmatrix} = \begin{bmatrix} M_1(s) \\ M_2(s) \\ M_3(s) \\ \vdots \\ M_N(s) \end{bmatrix}. \tag{39}$$

Any transfer function between any input $M_i(s)$ and any output $\theta_i(s)$ can be obtained by solving this set of equations. This is probably the most natural, and the easiest to use, modeling method for a multi-link system. Actually it coincides with the spectral finite element method [3], once one makes the substitution $s = \mathrm{j}\omega$. The structure of the model (39), as well as that of Eqs. (34) and (35), enables derivation of control laws for stabilization and tracking [18].

6. Conclusion

A method of transfer function modeling for multi-link flexible systems, governed by the wave equation, is presented. First a closed form expression for the transfer function of a single link is derived and analyzed. The building blocks of the transfer function are time delays, representing the wave motion, and low-order rational expressions, representing the boundary phenomena. Comparing the transfer function to finite dimension approximations reveals some advantages. Unlike modal models, the method handles lumped damping elements at the ends in a natural manner, and unlike FEM it gives the exact poles as the roots of its denominator. Even more fundamental is the explicit recognition of the wave motion and reflection as the principal mechanism of the response. This well-known fact is heavily masked, practically absent, in FEM and modal models. The transfer function approach leads naturally to accurate, yet simpler than solving PDEs, simulation schemes consisting of low-order linear blocks and delays. From a strict mathematical point of view the scheme is still infinite dimensional because of the delays, however in practice this is a standard block in many simulation software packages. Another application where the transfer function model is advantageous is feedback control design. Besides being the natural form of model for that task, the specific structure of the transfer function leads to control laws that eliminate the delay from the closed loop. The wave-delay correspondence implies that the control law makes the actuating end a sink for the returning wave.

The transfer function modeling method is extended to structures with multiple links, where three methods of constructing the multi-link model are discussed. The better ones seem to be the feedback approach and the infinite dimension equivalent of a "dynamic stiffness matrix". These methods provide a systematic way of assembling any number of single link transfer functions into a large multi-link model. As in the single link case, the multi-link transfer functions allow physical insight into the system, and the usefulness of the approach for classical vibration analysis, control synthesis and simulation is demonstrated.

Appendix A. Detailed derivation of the transfer function $G(x, x0, s)$

The first step is showing that Eq. (5) is indeed the solution of Eq. (3). It is easily seen that at any $x \neq x_0$, $\theta(x, s)$ can be written as

$$\theta(x,s) = \bar{C}_1(s)e^{sx/c} + \bar{C}_2(s)e^{-sx/c}, \tag{A.1}$$

which is identical with the homogeneous solution only with different coefficients. Hence at $x \neq x_0$ the left-hand side is equal to zero, same as the right-hand side. Notice now that

$$\frac{\partial\theta(x,s)}{\partial x} = \begin{cases} -\frac{M(s)}{4GI_p}(e^{s(x-x_0)/c} + e^{-s(x-x_0)/c}) + \frac{s}{c}(C_1(s)e^{sx/c} - C_2(s)e^{-sx/c}), & x > x_0, \\ \frac{M(s)}{4GI_p}(e^{s(x-x_0)/c} + e^{-s(x-x_0)/c}) + \frac{s}{c}(C_1(s)e^{sx/c} - C_2(s)e^{-sx/c}), & x < x_0. \end{cases} \tag{A.2}$$

Evaluating these expressions near x_0 yields

$$\frac{\partial\theta(x,s)}{\partial x} = \begin{cases} -\frac{M(s)}{2GI_p} + \frac{s}{c}(C_1(s)e^{sx_0/c} - C_2(s)e^{-sx_0/c}), & x = x_0^+, \\ \frac{M(s)}{2GI_p} + \frac{s}{c}(C_1(s)e^{sx_0/c} - C_2(s)e^{-sx_0/c}), & x = x_0^-. \end{cases} \tag{A.3}$$

Hence

$$\frac{\partial\theta}{\partial x}(x_0^+, s) - \frac{\partial\theta}{\partial x}(x_0^-, s) = -\frac{M(s)}{GI_p}. \tag{A.4}$$

That jump is translated to a delta function in the second derivative with the same magnitude as the right-hand side of Eq. (3). Substituting Eq. (5) into the boundary conditions (4) gives, after rearranging

$$b_2(s)C_1(s) + b_1(s)C_2(s) = \frac{M(s)}{4\phi s}(b_1(s)e^{sx_0/c} - b_2(s)e^{-sx_0/c}), \tag{A.5}$$

$$b_3(s)e^{sL/c}C_1(s) + b_4(s)e^{-sL/c}C_2(s) = \frac{M(s)}{4\phi s}(b_3(s)e^{s(L-x_0)/c} - b_4(s)e^{-s(L-x_0)/c}). \tag{A.6}$$

Here

$$b_1(s) = A_1(s) + \phi s, \quad b_2(s) = A_1(s) - \phi s, \quad b_3(s) = A_2(s) + \phi s, \quad b_4(s) = A_2(s) - \phi s$$

and ϕ and $A_i(s)$ were already defined. Eqs. (A.5) and (A.6) are linear in $C_1(s)$ and $C_2(s)$, and their solution is

$$C_1(s) = \frac{M(s)}{4\phi s}\frac{b_1(s)b_3(s)e^{s(L-x_0)/c} + b_2(s)b_4(s)e^{-s(L+x_0)/c} - 2b_1(s)b_4(s)e^{-s(L-x_0)/c}}{b_1(s)b_3(s)e^{sL/c} - b_2(s)b_4(s)e^{-sL/c}}, \tag{A.7}$$

$$C_2(s) = \frac{M(s)}{4\phi s}\frac{b_1(s)b_3(s)e^{s(L+x_0)/c} + b_2(s)b_4(s)e^{-s(L-x_0)/c} - 2b_2(s)b_3(s)e^{s(L-x_0)/c}}{b_1(s)b_3(s)e^{sL/c} - b_2(s)b_4(s)e^{-sL/c}}. \tag{A.8}$$

Dividing the numerator and the denominator of each expression by $b_1(s)b_3(s)e^{sL/c}$ and defining (same as Eq. (7))

$$R_1(s) = -\frac{b_2(s)}{b_1(s)}, \quad R_2(s) = -\frac{b_4(s)}{b_3(s)}.$$

$C_1(s)$ and $C_2(s)$ can be written as

$$C_1(s) = \frac{M(s)}{4\phi s}\frac{e^{-x_0 s/c} + R_1(s)R_2(s)(s)e^{-(2L+x_0)s/c} + 2R_2(s)(s)e^{-(2L-x_0)s/c}}{1 - R_1(s)R_2(s)e^{-2Ls/c}} \tag{A.9}$$

$$C_2(s) = \frac{M(s)}{4\phi s}\frac{e^{x_0 s/c} + R_1(s)R_2(s)e^{-s(2L-x_0)/c} + 2R_1(s)e^{-x_0 s/c}}{1 - R_1(s)R_2(s)e^{-2Ls/c}}. \tag{A.10}$$

Substituting Eqs. (A.9) and (A.10) into Eq. (5) yields the two cases in Eq. (6).

Appendix B. Vibration oriented properties of the transfer function (6)

This appendix contains a series of results that prove the statements given in Section 3 regarding the stability and poles location of the transfer function.

Observation 1. $|R_i(s)| \leqslant 1$ for every s in the ORHP with equality only for a free end where $R_i(s) \equiv 1$. $|R_i(\mathrm{j}\omega)| = 1$ for $\omega \neq 0$ if and only if $D_i = 0$.

Proof. Let $s = a + bj$, then

$$|R_i(s)| = \frac{[J_i(a^2+b^2) + (D_i - \phi)a + K_i] + [2J_iab + D_ib - \phi b]j}{[J_i(a^2+b^2) + (D_i + \phi)a + K_i] + [2J_iab + D_ib + \phi b]j}. \tag{B.1}$$

Straightforward calculation lead to

$$|\mathrm{Num}(R_i)|^2 - |\mathrm{Den}(R_i)|^2 = -4a\phi J_i(a^2+b^2) - 4\phi D_i(a^2+b^2) - 4a\phi K_i, \tag{B.2}$$

where 'Num' and 'Den' denote the numerator and denominator, respectively. Unless $J_i = K_i = D_i = 0$, expression (B.2) is negative for all $a > 0$, hence $|R_i(s)| < 1$. When $a = 0$, the left-hand side of Eq. (B.2) is zero if and only if $D_i = 0$.

Result a. The system does not have poles in the ORHP.

Proof. If $\mathrm{Re}(s) > 0$, then $|\exp(-2\tau s)| < 1$. From Observation 1 it follows that $|R_1(s)R_2(s)| \leqslant 1$, therefore s in the ORHP cannot be a solution of the characteristic equation (17).

Result b. The system has poles on the imaginary axis (except for the origin) if and only if $D_1 = D_2 = 0$ (this result, together with Result a are equivalent to (b) in Section 3.2).

Proof. Since $|\exp(-2\tau \mathrm{j}\omega)| = 1$, a pole on the imaginary axis requires that $|R_1(\mathrm{j}\omega)R_2(\mathrm{j}\omega)| = 1$. However from Eq. (B.2), $|R_i(\mathrm{j}\omega)| \leqslant 1$ with equality only when $D_i = 0$, hence 'only if'. If $D_1 = D_2 = 0$, $|R_1(\mathrm{j}\omega)R_2(\mathrm{j}\omega)| = 1\,\forall\omega$, hence $s = \mathrm{j}\omega$ is a pole for every ω satisfying the angle equation (18).

Result c. If $D_1 = D_2 = 0$ all the poles of the system are on the imaginary axis.

Proof. First notice that in the absence of damping, $R_i(s) = 1/R_i(-s)$. Let s^* be a solution of the characteristic equation (17). Then

$$R_1(s^*)R_2(s^*)\mathrm{e}^{-2\tau s^*} = 1. \tag{B.3}$$

Leading to

$$R_1(-s^*)R_2(-s^*)\mathrm{e}^{-2\tau(-s^*)} = \frac{1}{R_1(s^*)R_2(s^*)\mathrm{e}^{-2\tau s^*}} = 1. \tag{B.4}$$

Hence $-s^*$ is a pole as well. Since no poles exist in the ORHP, all the poles must reside on the imaginary axis.

References

[1] K.F. Graff, *Wave Motion in Elastic Solids*, Clarendon Press, Oxford, 1975.
[2] F. Fahy, *Sound and Structural Vibration*, Academic Press, New York, 1985.
[3] J.F. Doyle, *Wave Propagation in Structures*, Springer, New York, 1997.
[4] L. Meirovitch, *Dynamics and Control of Structures*, Wiley, New York, 1990.

[5] Y. Yong, Y.K. Lin, Propagation of decaying waves in periodic and piecewise periodic structures of finite length, *Journal of Sound and Vibration* 129 (1989) 99–118.
[6] B. Wie, On Modeling and Control of Flexible Space Structures, PhD Dissertation, Department of Aeronautics and Astronautics, Stanford University, 1981.
[7] A.G. Butkovskiy, *Green's Functions and Transfer Functions Handbook*, Ellis Horwood Limited, Chichester, UK, 1982.
[8] A.G. Butkovskiy, *Structural Theory of Distributed Systems*, Ellis Horwood Limited, Chichester, UK, 1983.
[9] J.W. Nicholson, L.A. Bergman, Free vibration of combined dynamical systems, *Journal of Engineering Mechanics* 112 (1) (1985) 1–13.
[10] L.A. Bergman, J.W. Nicholson, Forced vibration of combined dynamical systems, *Journal of Vibration, Acoustics, Stress, and Reliability in Design* 107 (1985) 275–281.
[11] J.W. Nicholson, L.A. Bergman, On the efficacy of the modal series representation for the Green function of vibrating continuous structures, *Journal of Sound and Vibration* 98 (1985) 299–304.
[12] B. Yang, C.A. Tan, Transfer functions of one dimensional distributed parameter systems, *ASME Journal of Applied Mechanics* 59 (1991) 1009–1014.
[13] C.A. Tan, B. Kang, Wave reflection and transmission in an axially strained, rotating Timoshenko shaft, *Journal of Sound and Vibration* 213 (1998) 483–510.
[14] A.H. von Flotow, Disturbance propagation in structural networks, *Journal of Sound and Vibration* 106 (1986) 433–450.
[15] K. Matsuda, Y. Kanemitsu, S. Kijimoto, A wave-based controller design for general flexible structures, *Journal of Sound and Vibration* 216 (2) (1998) 269–279.
[16] N. Raskin, Y. Halevi, Control of flexible structures governed by the wave equation, *Proceedings of the American Control Conference*, Arlington, VA, June 2001.
[17] N. Raskin, Y. Halevi, Rate feedback control of free–free uniform flexible rod, *Journal of Guidance, Control and Dynamics* 24 (2001) 1037–1040.
[18] Y. Halevi, C. Wagner-Nachshoni, Feedback control of flexible structures with non-uniform rods, *Proceedings of the American Control Conference*, Denver, CO, 2003, pp. 2646–2651.
[19] Y. Halevi, Control of flexible structures governed by the wave equation using infinite dimensional transfer functions, *ASME Journal of Dynamic Systems, Measurement, and Control* 127 (2005) 579–588.
[20] W.J. O'Connor, Wave-echo position control of flexible systems: towards an explanation and theory, *Proceedings of the American Control Conference*, Boston, MA, 2004.
[21] D.J. Inman, *Engineering Vibration*, Prentice-Hall, New Jersey, 2000.
[22] D.J. Mead, Waves and modes in finite beams: application of the phase-closure principle, *Journal of Sound and Vibration* 171 (1994) 695–702.
[23] F. Fahroo, Optimizing the decay rate in the damped wave equation: a numerical study, *Proceedings of the American Control Conference*, Denver, CO, 2003.
[24] L. Silverberg, Uniform damping control of spacecraft, *Journal of Guidance and Control and Dynamics* 9 (1986) 221–227.
[25] T. Furukawa, E. Shimemura, Predictive control for systems with time delay, *International Journal of Control* 37 (1983) 399–412.
[26] B.B. King, Modeling and control of a multiple component structure, *Journal of Mathematical Systems, Estimation and Control* 4 (1994) 1–36.